Available online at www.sciencedirect.com

SciVerse ScienceDirect

Ceramics International 38 (2012) 5139–5144

CERAMICS INTERNATIONAL

www.elsevier.com/locate/ceramint

Combustion synthesis and characteristics of aluminum oxynitride ceramic foams

Yongting Zheng *, Hongbo Li, Wei Zhou, Xiaonan Zhang, Guorui Ye

Center for Composite Materials and Structures, Harbin Institute of Technology, Harbin 150001, China

Received 10 January 2012; received in revised form 6 March 2012; accepted 6 March 2012
Available online 14 March 2012

Abstract

Aluminum oxynitride (AlON) ceramic foams were prepared by combustion synthesis using Al and Al_2O_3 as starting materials under high nitrogen pressure. By introducing $Al(NO_3)_3{\cdot}9H_2O$ into reactants as active pore-forming agent, AlON ceramic foams with well-distributed pores were cost-effectively fabricated. The influences of $Al(NO_3)_3{\cdot}9H_2O$ content on the combustion process, pore content and structure were studied systematically. The experiment results showed that porous AlON ceramics containing evenly distributed and noncontiguous pores were obtained when $Al(NO_3)_3{\cdot}9H_2O$ content was 30%, in which the closed porosity of 80% was found by Archimedes' method. Pore distribution measured by mercury intrusion porosimetry indicated that pores with several types of diameter were formed in the foams because of the different conditions of pore fusion and molten viscosity.

Keywords: B. Porosity; D. Al_2O_3; E. Structural applications

1. Introduction

Aluminum oxynitride (AlON), as a solid solution of AlN and Al_2O_3, has the advantages of good high temperature properties, thermal shock and oxidative resistance and chemical inertness [1–3], which make it an ideal candidate for a variety of applications under high temperatures. So AlON ceramic is attracted by many researchers, and has been prepared by various methods, such as hot-press sintering [4], carbothermal reduction [5,6], solid phase reaction [7], self-propagating combustion [8], spark plasma sintering (SPS) [9], microwave reactive sintering [10], and so on. However, AlON foam, which can be used in the field of molten metal filter, catalyst carriers and high-temperature thermal-insulation components, has seldom been studied systematically. High porosity (70–90%) and low density (0.3–0.6 g/cm^3) are the main characteristics of the ceramic foams, and the common preparation methods include the addition of pore-forming agent, foaming process, polymeric sponge impregnation and sol–gel process [11–14]. These preparation methods are highly involved and complicated to fabricate foam ceramics, resulting in low productivity, high costs and manufacturing problems during scale-up.

Combustion synthesis (CS) (self-propagating high temperature synthesis, SHS) provides a cheap and efficient method for the manufacture of inorganic refractory materials due to the advantages of high reaction temperatures, fast heating rates, short reaction times and no external power supply. AlON ceramics have been prepared by combustion synthesis under low air pressure using Al and Al_2O_3 powder as starting materials [8,15–17]. However, only a few papers have reported the preparation of AlON foam ceramics by combustion synthesis [18]. In this experiment, gas–solid combustion synthesis was adopted to prepare AlON foam ceramic. Due to the characteristic features of gas–solid combustion process, the products prepared by this process are typically porous, and the manufacturing process is energy saving and cost effective. By adding pore-foaming agent of $Al(NO_3)_3{\cdot}9H_2O$, the porosity of the foam ceramic can improved obviously.

In this study, foam AlON ceramics with high porosity and well-distributed pores were prepared by combustion synthesis, and the effects of active pore-forming agent of $Al(NO_3)_3{\cdot}9H_2O$ on the combustion synthesis process and foam structure were studied in detail.

* Corresponding author. Tel.: +86 451 86402392; fax: +86 451 86402392.
E-mail address: zhengyt@hit.edu.cn (Y. Zheng).

0272-8842/$36.00.
doi:10.1016/j.ceramint.2012.03.018

2. Experimental procedure

Raw materials used in this experiment included Al powder (free Al > 98%, average grain size is 6 μm, Fine materials Corp. Xi'an, China); α-Al_2O_3 (purity ≥ 99.99%, average grain size is 2 μm, Dalian Rall Fine Ceramic Co., LTD., China) and pore-foaming agent $Al(NO_3)_3{\cdot}9H_2O$ (purity > 99.9%, analytical reagent). After dried for 12 h at 60 °C, the powder mixture was processed by mechanical ball milling for 24 h with the ball to powder mass ratio of 3:1. The thoroughly mixed powder was uniaxially pressed to cylindrical shape with a diameter of 24 mm and relative density of 60%.

The combustion synthesis reaction in this study can be expressed as follows:

$$\mathrm{Al} + \mathrm{Al_2O_3} + \mathrm{Al(NO_3)_3} + \mathrm{N_2} \rightarrow \mathrm{AlON(foam)} + Q \quad (1)$$

where Q is the heat released by the exothermic chemical reaction. In above reaction, $Al(NO_3)_3{\cdot}9H_2O$ was not only used as a strong oxidizer to participate in reaction, but also as pore-forming agent to produce pore structure in the product. The reactant composition in this experiment was shown in Table 1.

AlON foam ceramic was synthesized under 100 MPa N_2 pressure in the super-high pressure SHS reactor. The roughcast was placed into the combustion chamber of the SHS reactor and ignited by a Ni–Cr resistance coil at the top of the sample. Once an electrical current flows through the ignition coil, the Ni–Cr coil generates enough heat to ignite the self-sustained combustion reaction.

The temperature profile of the combustion reaction was recorded by an *X–Y* recorder through the potential difference obtained by W–5%Re/W–26%Re thermocouples inserted in the bottom center at a depth of 10 mm. Specimens were machined into required shape by inside diameter slicer. X-ray diffraction analysis was conducted on the X-ray diffraction device (Rigaku *D*/max-rB, Japan). The morphology of the products was observed by scanning electron microscopy (SEM, S4700 and FEI Quanta 2000F). Porosity of the foam ceramics was measured by mercury intrusion method (AUTOPORE 9420, Micromeritcs, USA).

3. Results and discussion

3.1. Reaction temperature

The powder compacts can be ignited easily under high nitrogen pressure and the combustion wave front propagated throughout the sample with high temperature and velocity. Fig. 1 shows the effect of $Al(NO_3)_3{\cdot}9H_2O$ content on the temperature of combustion synthesis. With the increasing contents of $Al(NO_3)_3{\cdot}9H_2O$ foam agent, the volume of decomposed gas increased, and thus Al powder in reactant can reacted entirely, and combustion temperature improved accordingly. The combustion temperature, ranging from 2165 °C to 2650 °C, was higher than the melting point of Al_2O_3 (2065 °C) and AlN (2150 °C, sublimating point). These molten phases, which existed in combustion reaction zone, can affect the foam structure in the ceramics. Combustion synthesis is a rapid process and only last for several to 10 s in the experiments. Although the operational temperature of the W–5%Re/W–26%Re thermocouples is under 2300 °C for working conditions, its instantaneous working temperature can reach 2800 °C.

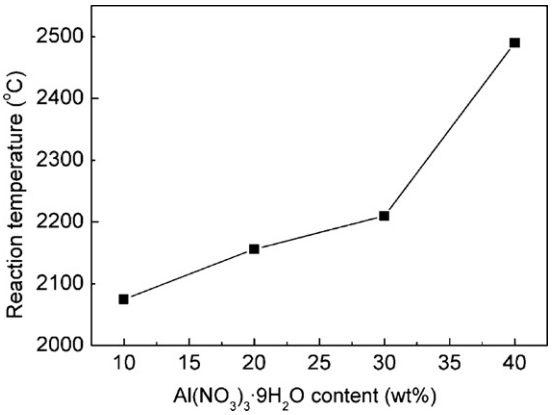

Fig. 1. Effect of $Al(NO_3)_3{\cdot}9H_2O$ content on the temperature of the combustion synthesis.

Table 1
Composition of the reactant used in the experiment.

Samples	$Al(NO_3)_3{\cdot}9H_2O$ (wt%)	Al (wt%)	Al_2O_3 (wt%)
A	10	40	50
B	20	40	40
C	30	40	30
D	40	40	20

Reaction (1) is an overall chemical process for the preparation of porous AlON ceramic, and it involves the following reactions.

At 110 °C, the dehydration reaction of the $Al(NO_3)_3{\cdot}9H_2O$ occurs:

$$\mathrm{Al(NO_3)_3{\cdot}9H_2O(g)} = \mathrm{Al(NO_3)_3} + 9\mathrm{H_2O} \quad (2)$$

When heated above 500 °C, the following reaction takes place:

$$2\mathrm{Al(NO_3)_3} = \mathrm{Al_2O_3} + 3\mathrm{N_2} + \frac{15}{2\mathrm{O_2}} \quad (3)$$

Reaction between Al and oxygen is prior to the reaction between Al and nitrogen because of the higher oxidability of oxygen than nitrogen:

$$\mathrm{Al} + \frac{3}{4}\mathrm{O_2} = \frac{1}{2}\mathrm{Al_2O_3} \quad (4)$$

The residual Al is reacted with nitrogen:

$$\mathrm{Al} + \frac{1}{2}\mathrm{N_2} = \mathrm{AlN} \quad (5)$$

At last, the solid solution reaction between Al_2O_3 and AlN happened to form AlON at the high combustion temperature:

$$(x+5y)\mathrm{AlN} + (2x+y)\mathrm{Al_2O_3} \rightarrow x\mathrm{Al_5O_6N} + y\mathrm{Al_7O_3N_5} \quad (6)$$

Once the combustion synthesis begins after the ignition, the exothermic reactions of Eq. (4) ($\Delta H = -1675$ kJ/mol) and

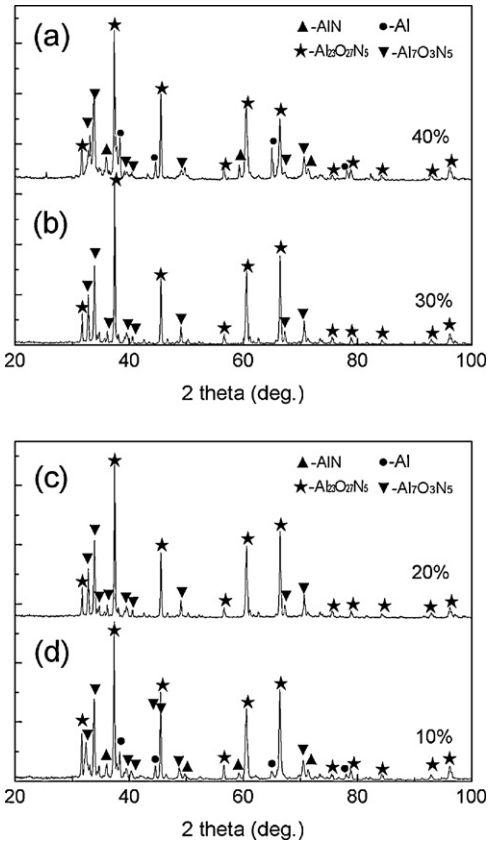

Fig. 2. X-ray diffraction patterns of the SHS products with different $Al(NO_3)_3{\cdot}9H_2O$ contents.

Eq. (5) ($\Delta H = -318$ kJ/mol) released enough heat to sustain the reaction propagation. The decomposition of $Al(NO_3)_3{\cdot}9H_2O$ and subsequent decomposition of $Al(NO_3)_3$, which form the water vapor, nitrogen and oxygen, can produce the foam structure and also provide nitrogen and oxygen to form Al_2O_3 and AlN. Due to the different content of Al_2O_3 and AlN, different O/N ratio in AlON phase was found in this experiment. At the same time, the massive gas decomposed from $Al(NO_3)_3{\cdot}9H_2O$ can produce high pressure and result in the breakdown of the foam structure, so high nitrogen pressure guaranteed the pressure balance to form good foam structure in the product.

3.2. Phase composition

The XRD patterns of the products with different $Al(NO_3)_3{\cdot}9H_2O$ content were shown in Fig. 2. A small trace of residual Al and AlN was found in sample A and sample B. AlON phase in the products was mainly composed of $Al_{23}O_{27}N_5$ (γ-AlON) and $Al_7O_3N_5$. Usually, spinel γ-AlON is the preferable stable phase in traditional fabrication process because of the long holding time and slow cooling rate [1,19]. However, during the rapid combustion synthesis in this experiment, AlON phase has no sufficient time to evolve completely to stable spinel phase, and a certain amount of $Al_7O_3N_5$ ($Al_2O_3{\cdot}5AlN$) formed instead [17].

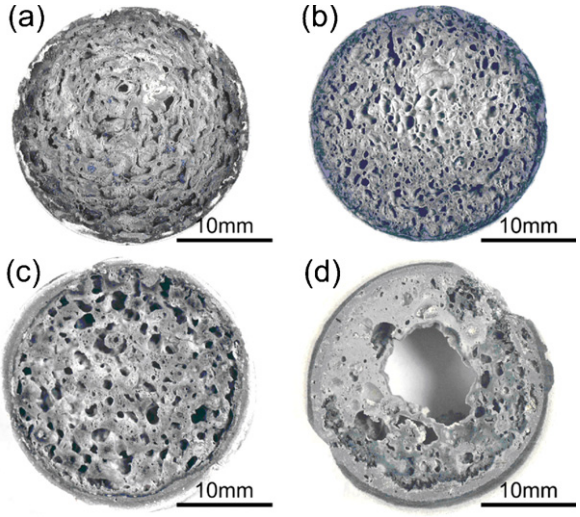

Fig. 3. Optical morphological differences of the products with different $Al(NO_3)_3{\cdot}9H_2O$ contents: (a) 10%; (b) 20%; (c) 30%; (d) 40%.

When $Al(NO_3)_3{\cdot}9H_2O$ content was 10% and 20%, the production of decomposed gas was relatively small and the reaction carried out incompletely, so small amount of Al remained in the products. At the same time, relative lower combustion temperature hindered the formation of AlON solid solution, so small trace of AlN was observed in the product when $Al(NO_3)_3{\cdot}9H_2O$ content was 10% and 20%.

When $Al(NO_3)_3{\cdot}9H_2O$ content was 30% and 40%, the reaction can take place thoroughly. Since the sample with $Al(NO_3)_3{\cdot}9H_2O$ content of 30% and 40% can produce more oxygen gas comparing to that of 10% and 20% content, and what is more, oxygen was more active than nitrogen, there was more Al_5O_6N ($2Al_2O_3{\cdot}AlN$) phase that contained higher oxygen content in the product, as shown in Fig. 2(c) and (d).

3.3. Pore structure

The $Al(NO_3)_3{\cdot}9H_2O$ content has also a critical effect on the pore structure of the products. Fig. 3 shows the pores of the products with different $Al(NO_3)_3{\cdot}9H_2O$ contents. When $Al(NO_3)_3{\cdot}9H_2O$ content was 10%, the reaction cannot produce sufficient gas to form pore structure, as shown in Fig. 3(a). This was attributed to the lower reaction temperature, higher solid phase fraction and less decomposed gas. While the $Al(NO_3)_3{\cdot}9H_2O$ content increased to 20%, the reaction temperature, liquid phase and decomposed gas increased, and high porosity product with uniform closed pore distribution was obtained. When $Al(NO_3)_3{\cdot}9H_2O$ content reached 30%, the reaction temperature and liquid content were more higher, viscous resistance decreased and the content of decomposed gas increased, and all the above factors are favorable for the pore formation. At the same time, the driving force of pore fusion was also larger, so the pore fusion was obvious, which result in the formation of larger diameter pores, as shown in Fig. 3(c). When $Al(NO_3)_3{\cdot}9H_2O$ content was 40%, large pore was formed in the middle of the product due to the higher temperature and more pore fusion in the interior sample; while

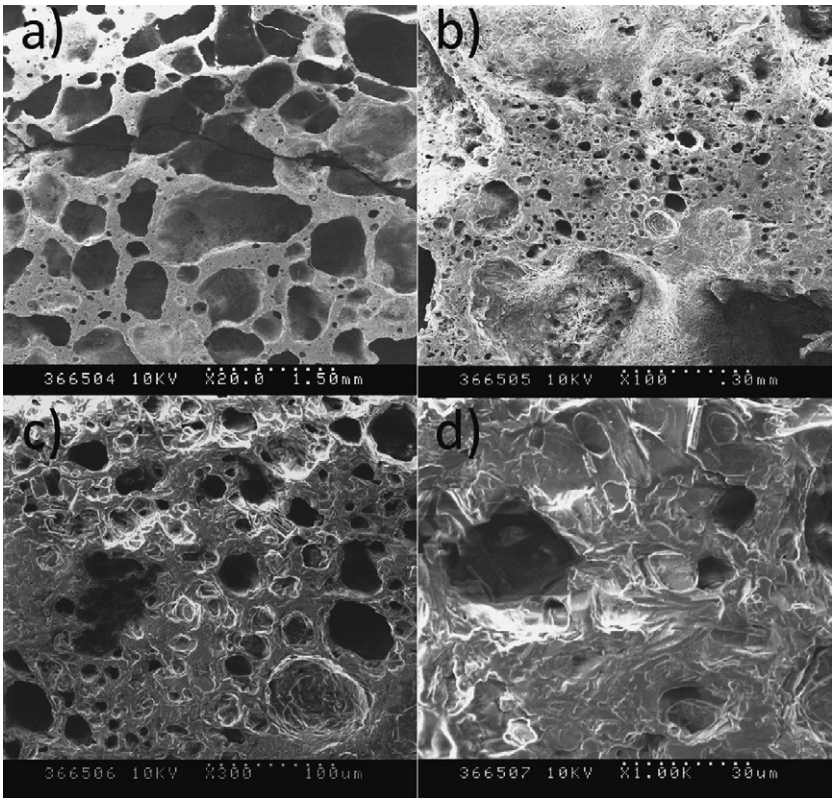

Fig. 4. SEM images of pore in sample B (20%): (a) large pores; (b) pore wall; (c) pores in the wall; and (d) amplification of the pores in the wall.

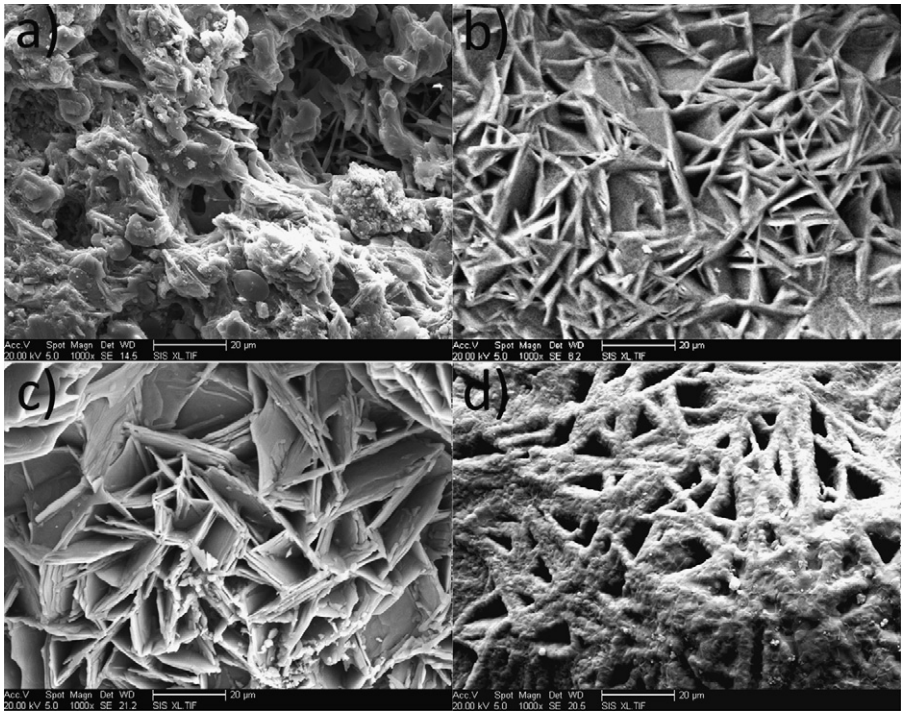

Fig. 5. Microstructure of the pore inner surface of the samples with $Al(NO_3)_3{\cdot}9H_2O$ contents of: (a) 10%; (b) 20%; (c) 30%; and (d) 40%.

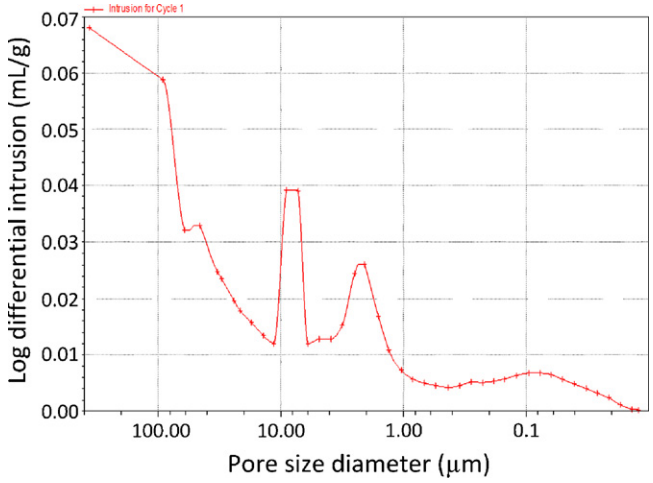

Fig. 6. Aperture distribution of the sample B by mercury intrusion method.

relative small pores were observed near to the surface due to relative lower temperature of the sample surface.

3.4. Formation mechanism and characteristics

Fig. 4 shows the SEM images of the pores and pore walls at different magnification in sample B. As the figure indicated, the average size of the pores was found to be about 0.5–1.5 mm, and the average thickness of the pore walls was 0.1–0.3 mm. In addition, the pores were not exactly the spherical shape, especially the pores with medium diameter, and the adjacent angle of 60° or 120° between the two conterminal walls was observed, as shown in Fig. 4(a). This was attributed to the pore size and viscosity of the molten alloys at high temperature. Pores formed during combustion process were relatively easy to move and merge together to form larger pores because the higher viscosity of the molten phases at high temperatures, and the pore walls, which were relatively thinner than the size of the pores, were readily to change their shape to balance the pressure of the pores. So the constant angles between adjacent walls were formed when pressure in the pores was in equilibrium. Besides the large pores in the products, small pores with diameter of about 50 μm in pore walls were observed, as shown in Fig. 4(b) and (c). Because of the small size and higher viscosity, these pores remained in the walls and kept the spherical shape. Fig. 4(d) shows the microstructure of the small pores in the pore walls.

Fig. 5 shows the microstructure morphologies of the pore inner surface of the samples with different $Al(NO_3)_3{\cdot}9H_2O$ contents. Interlaced flake microstructure was observed in the products. According to the reaction temperature shown in Fig. 1, the temperature increased with the increasing content of $Al(NO_3)_3{\cdot}9H_2O$. Few interlaced microstructure was found in smple A becasue of the low reaction temperature. With the increasing of the reaction temperature, large amount of interlaced microstructure was observed, and higher reation temperature promoted the growth of the interlaced microstructure, as shown in Fig. 5(b) and (c). The formation of the interlaced microstructure increased effectively the surface area of the pores, and improved the porosity of the ceramic foams. In sample D shown in Fig. 5(d), the interlaced structure presented molten state because the reaction temperature was too high for the ceramic foam.

Fig. 6 shows the pore distribution of the sample B measured by mercury porosimetry. Large pores with diameter >100 μm were dominant in the ceramic foam. There were several fluctuations on the curve which occurred in pore diameter of 50 μm, 8 μm, 2 μm and 0.1 μm, which was in accordance with the analysis results based on Figs. 4 and 5. Pore distribution of the ceramic foam was divided into several types of diameter. Fig. 7 presents the specific area of sample B measured by mercury intrusion method. The changes on the curve of specific area verified the variation on pore distribution in Fig. 6.

3.5. Porosity of the products

On the basis of above analysis, the reaction temperature and decomposed gas content increased with the increasing of

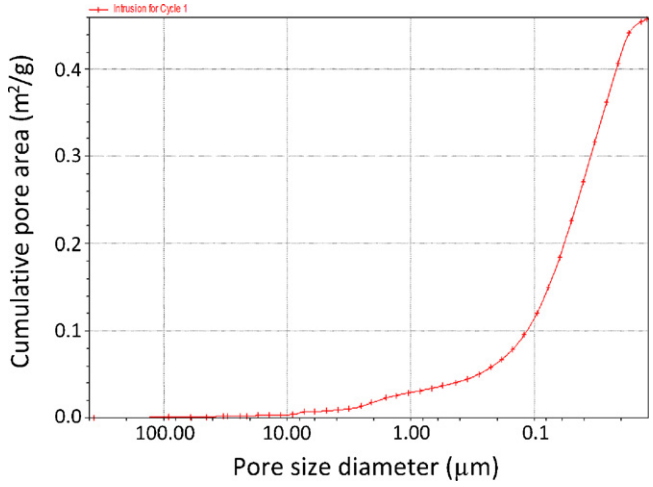

Fig. 7. Integral curves of specific area of sample B by mercury intrusion method.

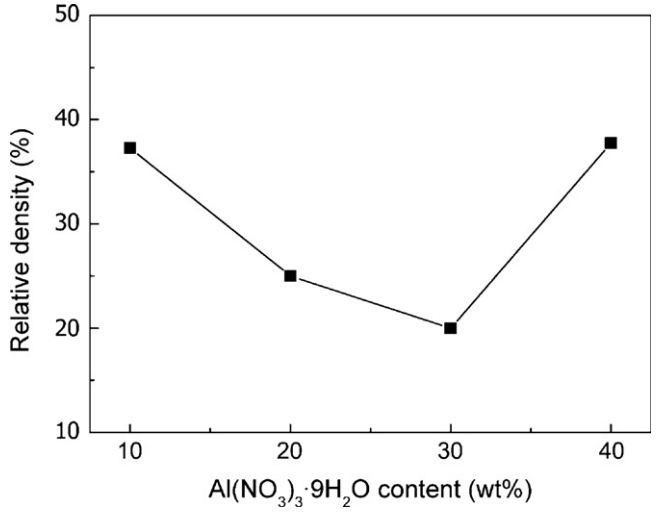

Fig. 8. Effect of $Al(NO_3)_3{\cdot}9H_2O$ content on the relative density of the products.

$Al(NO_3)_3{\cdot}9H_2O$ content, which was beneficial to improve the porosity of products. When the combustion reaction produced appropriate liquid phase with lower viscous resistance at $Al(NO_3)_3{\cdot}9H_2O$ content of 20 and 30%, foam AlON ceramic with high porosity formed. On the other hand, when reaction temperature was too high at $Al(NO_3)_3{\cdot}9H_2O$ content of 40%, pore fusion and gas escaping cannot be controlled, so the porosity is decreased sharply. The effect of $Al(NO_3)_3{\cdot}9H_2O$ content on the relative density of the product was shown in Fig. 8. It can be found that the relative density of the foam ceramic decreased with increasing $Al(NO_3)_3{\cdot}9H_2O$ content, and reached minimum density of 20% at $Al(NO_3)_3{\cdot}9H_2O$ content of 30%. The formation of large open pore in the foam ceramic lead to the higher relative density at $Al(NO_3)_3{\cdot}9H_2O$ content of 40%.

4. Conclusions

Using $Al(NO_3)_3{\cdot}9H_2O$ as active pore-forming agent, AlON foam ceramic was fabricated by combustion synthesis reaction from powder compact of Al and Al_2O_3. Higher $Al(NO_3)_3{\cdot}9H_2O$ content led to higher reaction temperature and more decomposed gas production, which was beneficial to improve the porosity of products. The products with well-distributed pores was fabricated when $Al(NO_3)_3{\cdot}9H_2O$ content was 20% and 30%. When reaction temperature was too high for sample with $Al(NO_3)_3{\cdot}9H_2O$ content of 40%, pore fusion and gas escape cannot be controlled, and then the porosity is decreased. Pore distribution indicated that pores with several types of diameter were formed in the foams under different conditions of pore fusion and molten viscosity.

Acknowledgements

This work was supported by the National Natural Science Foundation of China (No. 91016014).

References

[1] N.D. Corbin, Aluminum oxynitride spinel: a review, J. Eur. Ceram. Soc. 5 (1989) 143–154.
[2] X.D. Wang, F.M. Wang, W.C. Li, Synthesis, microstructures and properties of γ-aluminum oxynitride, Mat. Sci. Eng. A 342 (2003) 245–250.
[3] S. Mandal, A.S. Sanyal, K.K. Dhargupta, S. Ghatak, Gas pressure sintering of β-SiC-γ-alon composite in nitrogen/argon environment, Ceram. Int. 27 (2001) 473–479.
[4] X.D. Wang, D. Sichen, W.C. Li, S. Seetharaman, Kinetic studies of the oxidation of γ-aluminum oxynitride, Metall. Mater. Trans. B 33 (2002) 201–207.
[5] J. Zheng, B. Forslund, Carbothermal synthesis of aluminium oxynitride (ALON) powder: influence of starting materials and synthesis parameters, J. Eur. Ceram. Soc. 15 (1995) 1087–1100.
[6] Y.W. Li, N. Li, R.Z. Yuan, Effect of raw materials on carbothermal reduction synthesis of γ-aluminum oxynitride spinel powder, J. Mater. Sci. 34 (1999) 2547–2552.
[7] S. Bandyopadhyay, G. Rixecker, F. Aldinger, S. Pal, K. Mukherjee, H.S. Maiti, Effect of reaction parameters on γ-AlON formation from Al_2O_3 and AlN, J. Am. Ceram. Soc. 85 (2002) 1010–1012.
[8] D. Zientara, M. Bucko, J. Lis, AlON-based materials prepared by SHS technique, J. Eur. Ceram. Soc. 27 (2007) 775–779.
[9] F.C. Sahin, H.E. Kanbur, B. Apak, Preparation of AlON ceramics via reactive spark plasma sintering, J. Eur. Ceram. Soc. 32 (2012) 925–929.
[10] J.P. Cheng, D. Agrawal, Y.J. Zhang, R. Roy, Microwave reactive sintering to fully transparent aluminum oxynitride (ALON) ceramics, J. Mater. Sci. Lett. 20 (2001) 77–79.
[11] H.X. Peng, Z. Fan, J.R.G. Evans, J.J.C. Busfield, Microstructure of ceramic foams, J. Eur. Ceram. Soc. 20 (2000) 807–813.
[12] J. Luyten, S. Mullens, J. Cooymans, A.M. De Wilde, I. Thijs, R. Kemps, Different methods to synthesize ceramic foams, J. Eur. Ceram. Soc. 29 (2009) 829–832.
[13] X.J. Mao, S. Shimai, S.W. Wang, Effects of coarse particles on the gelcasting of ceramic foams, J. Am. Ceram. Soc. 91 (2008) 2412–2414.
[14] J.F. Qiu, J.T. Lib, K.L. Smirnov, Combustion synthesis of high porosity SiC foam with nanosized grains, Ceram. Int. 36 (2010) 1901–1904.
[15] J. Lee, I. Lee, H. Chung, J. Ahn, D. Kim, B. Kim, Self-propagating high-temperature synthesis for aluminum oxynitride (AlON), Mater. Sci. Forum. 510–511 (2006) 662–665.
[16] A. Gromov, A. Ilyin, A. Ditts, V. Vereshchagin, Combustion of $Al–Al_2O_3$ mixtures in air, J. Eur. Ceram. Soc. 25 (2005) 1575–1579.
[17] J. Jung, S. Baik, Combustion synthesis of AlON–BN composites under low nitrogen pressure, J. Am. Ceram. Soc. 90 (2007) 3063–3069.
[18] Y.T. Zheng, X.F. Yun, X.K. Zhang, Fabrication and microstructure of AlON ceramic by self-propagating high-temperature synthesis and hot isostatic pressing, Mater. Sci. Technol. 16 (2008) 481–484.
[19] Y. Takao, M. Sando, Al-system non-oxide spherical powder synthesis by liquefied petroleum gas firing, J. Am. Ceram. Soc. 88 (2005) 450–452.